

## Recent advances in wireless epicortical and intracortical neuronal recording systems

Bowen JI<sup>1,2,3†</sup>, Zekai LIANG<sup>1,2†</sup>, Xichen YUAN<sup>2</sup>, Honglai XU<sup>4</sup>, Minghao WANG<sup>5</sup>,  
Erwei YIN<sup>6,7</sup>, Zhejun GUO<sup>8</sup>, Longchun WANG<sup>8</sup>, Yuhao ZHOU<sup>1,2,3</sup>,  
Huicheng FENG<sup>1,2</sup>, Honglong CHANG<sup>1,2\*</sup> & Jingquan LIU<sup>8\*</sup>

<sup>1</sup>Unmanned System Research Institute, Northwestern Polytechnical University, Xi'an 710072, China;

<sup>2</sup>Ministry of Education Key Laboratory of Micro and Nano Systems for Aerospace, School of Mechanical Engineering, Northwestern Polytechnical University, Xi'an 710072, China;

<sup>3</sup>Collaborative Innovation Center of Northwestern Polytechnical University, Shanghai 201108, China;

<sup>4</sup>NEURACLE TECH (China) Co., Ltd., Changzhou 213100, China;

<sup>5</sup>College of Electronics and Information, Hangzhou Dianzi University, Hangzhou 310018, China;

<sup>6</sup>Defense Innovation Institute, Academy of Military Sciences (AMS), Beijing 100071, China;

<sup>7</sup>Tianjin Artificial Intelligence Innovation Center (TAIIC), Tianjin 300450, China;

<sup>8</sup>National Key Laboratory of Science and Technology on Micro/Nano Fabrication, Department of Micro/Nano Electronics, Shanghai Jiao Tong University, Shanghai 200240, China

Received 9 August 2021/Revised 27 September 2021/Accepted 27 October 2021/Published online 10 March 2022

**Abstract** An implantable brain-computer interface (BCI) has proven to be effective in the field of sensory and motor function restoration and in the treatment of neurological disorders. Using a BCI recording system, we can transform current methods of human interaction with machines and the environment, especially to help those with cognitive and mobility disabilities regain mobility and reintegrate into society. However, most reported work has focused on a simple aspect of the whole system, such as electrodes, circuits, or data transmission, and only a very small percentage of systems are wireless. A miniature, lightweight, wireless, implantable microsystem is key to realizing long-term, real-time, and stable monitoring on freely moving animals or humans in their natural conditions. Here, we summarize typical wireless recording systems, from recording electrodes, processing chips and controllers, wireless data transmission, and power supply to the system-level package for either epicortical electrocorticogram (ECoG) or intracortical local field potentials (LFPs)/spike acquisition, developed in recent years. Finally, we conclude with our vision of challenges in next-generation wireless neuronal recording systems for chronic and safe applications.

**Keywords** wireless implant, neuronal recording system, recording electrodes, processing chips, wireless data transmission, power supply, system-level package

**Citation** Ji B W, Liang Z K, Yuan X C, et al. Recent advances in wireless epicortical and intracortical neuronal recording systems. *Sci China Inf Sci*, 2022, 65(4): 140401, <https://doi.org/10.1007/s11432-021-3373-1>

## 1 Introduction

The last decade has witnessed the rapid development of wireless implants for interaction with the brain. Compared to electrical, optical, or chemical modulation, neural recording is much more challenging due to highly complex procedures, including signal acquisition, amplification, filtering, digitization, transmission, and decoding [1–5]. Small numbers of neurons can provide massive information through electrophysiological recording technology and are promising for clinical applications over weeks, months, or even years. High-quality neural signals from either the epicortical or intracortical area can be used to translate neural activity to text [6, 7], operate robotic prostheses or wheelchairs [8–11], control an exoskeleton [12], and even restore body movement and sense of touch [13, 14]. Until now, most implants are tethered to commercial neural recording data acquisition systems (16 bits per sample at 30 kS/s per channel) with dozens

\* Corresponding author (email: changhl@nwpu.edu.cn, jqliu@sjtu.edu.cn)

† Authors Ji B W and Liang Z K have the same contribution to this work.

to one thousand channels, such as Plexon, Blackrock, NeuroNexus, Tucker-Davis Technologies, and Neuralynx. A wired table-top acquisition system is reliable and powerful, with no need to worry about weak signal transmission and processing, power consumption, or strict packaging of implants. However, wire connections to the system limit the range of free activity, increase the risk of infection, and constrain subjects from recording anytime and anywhere.

Wireless neuronal recording technology is one of the most important future trends because of the significant advantage of portable recording at any point in time and space [15]. This technology involves two aspects: wireless data transmission outward to terminal equipment and wireless power transmission into the neuronal recording system. For wireless data transmission, either epicortical or intracortical neural signals contain a large amount of data, especially in terms of continuous recording time and high channel count. Various wireless solutions have been used in animal studies in recent years, including radio frequency (RF) [16], ZigBee [17], Bluetooth [18], and WiFi [19], owing to the rapid development of wireless communication. For wireless power transmission, systems can either directly power the wireless neural interface or recharge batteries through an inductive link [20–23]. However, research of wireless neuronal recording is still in its infancy due to engineering challenges, and it therefore needs to balance low power consumption, high bandwidth, and real-time transmission. In addition, a fully implanted device might interfere with the wireless transmission of neural signals or affect its own lifetime in an intracranial environment. Consequently, the demand for developing high-performance wireless recording implants in free-behavior animals is high.

System-level integration can provide convenient operation and low-noise performance thanks to compact size, short interconnections, and wireless transmission. A miniature, lightweight, wireless, and implantable microsystem is key to realizing long-term, real-time, and stable monitoring on untethered animals in their natural conditions, including rodents [21,24], sheep [25], and non-human primates [18,26,27]. In 2021, a battery-powered wireless intracortical recording system was tested non-stop in two patients with paralysis over a 24-h period at home by BrainGate [28], which can transmit and recognize signals generated by individual neurons and support full high-bandwidth signal transmission. BrainGate provides the first wireless brain-computer interface (BCI) transmitter available to humans. The typical configuration of a wireless neuronal recording system consists of five modules, as illustrated in Figure 1. (1) Implantable electrodes for neural signal acquisition; (2) processing chips and a controller for signal amplification, filtering, multiplexing, digitization, and controlling the parameter setting; (3) wireless data transmission to a computer or other portable equipment for further data analysis; (4) power supply by wireless charging or an inductive coil for system power consumption; and (5) packaging for ultracompact size and long service life. To be ready for actual use, the trade-offs between channel count, power consumption, packaging size, compatibility, and lifetime should be carefully considered. In view of the above factors, wireless neuronal recording systems are rapidly developing toward miniaturization [24,29,30], integration [23,31,32], and intelligence [33–35], benefiting from micro-electromechanical systems (MEMS), integrated circuits (IC), wireless transmission and powering, and machine learning algorithms. Wireless neuronal recording systems can be not only applied in healthcare and interaction for people with severe motor impairment but also has future potential in entertainment and military scenarios.

This paper reviews the latest progress in wireless epicortical and intracortical neuronal recording systems in five closely linked subsections, including recording electrodes, processing chips and controllers, wireless data transmission, power supply, and packaging. Challenges facing these systems are also summarized to create a direct path for future long-term and reliable recording systems according to existing technical shortcomings.

## 2 Recording electrodes

Three types of electrical potentials can be recorded through intracortical neural interfaces: epicortical electrocorticogram (ECoG), intracortical local field potentials (LFPs), and action potentials (spikes) [36,37]. ECoGs are recorded from the epidural or subdural area closer to the cortical surface. Thus, implantation of ECoG electrodes only requires minimally invasive surgery, without intrusion into brain tissue [38]. As a comparison, penetrating electrodes can be used to record LFP and spikes with richer information from neurons but with higher invasive trauma. Examples include Utah arrays, Michigan probes, and microwires. An LFP is synchronized neuronal activity recorded from small populations of neurons by their extracellular potentials and has higher spatial resolution than ECoGs [39]. Spikes represent a se-

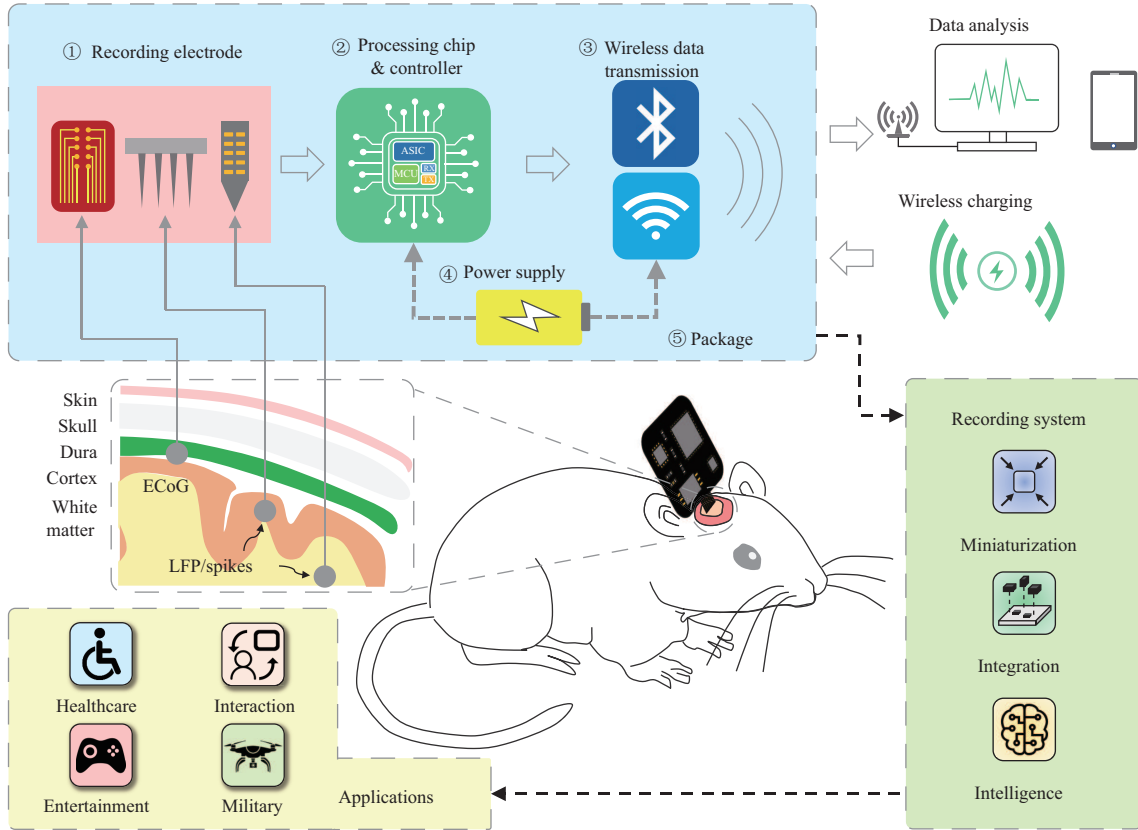


**Figure 1** (Color online) Configuration, trends, and applications of wireless epicortical and intracortical neuronal recording systems.

quence of short electrical pulses in the membrane potential of individual neurons, or a small neuronal group, compared to LFP [40]. The different properties of the latest recording electrode technologies are compared in Table 1 [32, 41–49].

### 2.1 ECoG electrode

ECoG electrodes have been used to locate the epileptic focus and decode movements, vision, and speech. From the size of the electrode site, ECoG electrodes fall into two basic categories: macro and micro. Traditional macro-ECoG electrodes, with site diameters of 1–4 mm and a pitch of  $\sim 1$  cm, are commercially available from Neupace, PMT Corp., Medtronic, WISE Srl, among others. Softer and thinner silicone-based macro-ECoG grids have been developed for better conformability to curved surfaces compared with clinical macro-ECoGs [41] (Figure 2(a)).

Current trends of miniaturization have pushed spatial resolution to less than 1 mm, namely to micro-ECoG electrodes. Latest work has mainly focused on stretchability for conformal contact to the brain surface [50, 51], transparency for optical imaging or resistance to artifacts [52, 53], multiplexing for high density [54, 55], and multifunction for customizable intracranial applications [56, 57]. Similar to silicone-based macro-ECoGs, an ultrasoft and stretchable micro-ECoG grid with  $50 \mu\text{m} \times 50 \mu\text{m}$  microelectrode sites has also become a hot topic [58] (Figure 2(b)).

### 2.2 Utah/Utah-like arrays

In 1989, a typical penetrating electrode, namely the Utah electrode array (UEA), was proposed by Richard Normann at the University of Utah [59]. With clinical approval by the Food and Drug Administration (FDA) and an implant lifetime of more than seven years, it is the most widely used, gold standard recording electrode for decoding minds and controlling external devices. A traditional UEA is composed of 100 three-dimensional needles in a  $10 \times 10$  configuration, 1.5-mm in length, with a  $400 \mu\text{m}$  pitch and  $4 \text{ mm} \times 4 \text{ mm}$  overall size. However, LFP/spikes can only be received from needle tips with set dimensions and parameters. In 2020, Shandhi and Negi [44] proposed a multisite UEA based on the traditional Utah

**Table 1** Comparison of different properties of novel recording electrode technologies

Ref. (Year)	Type	Name	Channels	Feature sizes	Materials	Implantation location	Chronic stability
[41] (2021)	Macro-ECoG electrode	Soft Grid	32	2.3 mm diameter; 5–10 mm pitch; 4 cm×10 cm coverage	PDMS substrate; Cr/Au interconnects; Pt nanoparticles on electrode sites	Above the somatosensory and motor cortex of minipig	2 weeks
[42] (2020)	Micro-ECoG electrode	Opto-E-Dura	16	Ring shaped electrode with an inner diameter of 200 μm and an outer diameter of 400 μm	PDMS substrate; gold nanowire (Au NW)tracks; platinum (Pt) particle electrodes	Above the dorsal cortex of mouse	6 weeks
[43] (2021)	Micro-ECoG electrode	–	1152 (128ch×9)	50 μm×50 μm electrode size; 295 μm pitch; 14 mm×7 mm coverage	Parylene-C substrate; gold signal tracks	Above the somatosensory cortex of macaque monkey	Acute
[44] (2020)	Utah array	UMEA	75–900 (3/9 sites per shaft)	One at the tip of shaft and two others about 300 μm and 450 μm below; 1.5 mm long shaft with 400 μm pitch	Silicon substrate; TiW and Pt as metal layer; Paylene-C encapsulation	In vitro	–
[45] (2021)	Utah-like array	Argo	65536 (256×256)	5 to 25 μm metal wires of diameters; 10 mm diameter microwire array	Platinum-iridium alloy in microwire cores; Parylene-C insulation	0.7–1 mm into the rat cortex and auditory cortex of sheep	Acute
[46] (2020)	Utah-like array	CHIME	100–1000	Electrodes with 22–25 μm OD and 1–7 μm ID; inter-wire spacing of around 100 μm	Glass-ensheathed gold microwires	Olfactory bulb of mouse	Acute
[47] (2018)	Michigan probe(stiff)	Neuropixels	960	12 μm×12 μm electrode size; 20 μm pitch; shank 70 μm×20 μm cross-section with 10 mm length	TiN as electrode sites; silicon substrate	Visual cortex, hippocampus, thalamus, motor cortex, striatum of mouse	Up to 60 days
[48] (2021)	Michigan probe(stiff)	Neuropixels 2.0	5120 (1280ch per shank)	12 μm×12 μm electrode size; 15 μm pitch; shank 70 μm×20 μm cross-section with 10 mm length	TiN as electrode sites; silicon substrate	Cortex, hippocampus, thalamus of mouse	Up to 309 days
[32] (2019)	Michigan probe (flexible)	Neuralink's threads	3072 (32ch per thread)	Probes with 32 electrode contacts spaced by 50/75 μm	Surface treatments: PEDOT/IrOx; substrate, encapsulation and dielectric of probe: polyimide; gold thin film trace	Unknown implantation location of rat	–
[49] (2019)	Michigan probe (flexible)	Neurotassels	128–1024	3 μm×1.5 μm cross-section; fibers total diameter of ~100 μm	Au microelectrodes encapsulated by polyimide; platinum electrodeposition	Medial prefrontal cortex of mouse	Up to 6 weeks

array, with nine sites per shaft, 900 active sites in total, and recording/stimulation capability from different cortex layers (Figure 2(c)). In 2021, Sahasrabuddhe et al. [45] proposed a Utah-like electrode array composed of 65536 channels of parallel platinum-iridium microwires bonded to a complementary

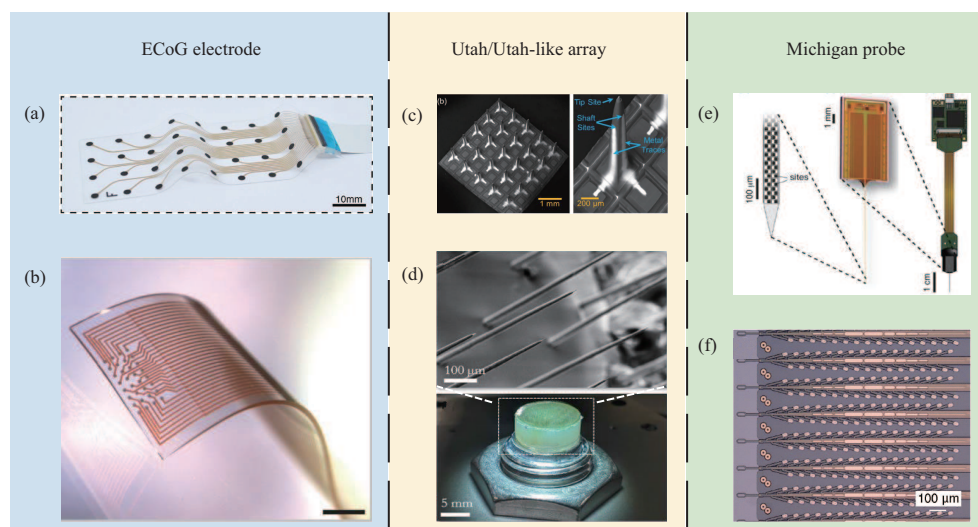


**Figure 2** (Color online) Typical epicortical and intracortical recording electrodes. (a) Macro-ECoG electrode array with a diameter of 2.3 mm and large coverage of 4 cm×10 cm [41] Copyright 2021 John Wiley and Sons. (b) Micro-ECoG electrode array with a size of 50 μm×50 μm and pitch of 200 μm. Scale bar: 1 mm [58] Copyright 2018 John Wiley and Sons. (c) Untraditional Utah array with nine sites per shaft and 900 microelectrode sites in total [44] Copyright 2020 IEEE. (d) Argo: Utah-like array with 65536 channels for high density recording [45] Copyright 2021 IOP Publishing. (e) Neuropixels: rigid silicon probe with 960 recording sites on a 70 μm×20 μm shank [47] Copyright 2018 Elsevier. (f) Neuralink's threads: flexible polyimide probes with 3072 electrode sites per array distributed across 96 threads (CC BY-ND 4.0) [32] Copyright 2019 Elon Musk, Neuralink.

metal-oxide-semiconductor (CMOS) voltage amplifier array (Figure 2(d)). This is the largest neural recording capability to date.

### 2.3 Michigan probe

Another typical penetrating electrode is the Michigan probe, which is based on a rigid silicon substrate to acquire LFP/spikes from individual neurons along the length of shanks rather than at the end (like a Utah array). Recent work has mainly focused on high density [60,61], flexibility [49,62], and multifunction [63–66]. Harris et al. [47] proposed multiplexed silicon probes based on CMOS technology named Neuropixels, with a 130-nm wire width, 10-mm shank length, and 960 recording sites on a 70 μm×20 μm shank (Figure 2(e)). They reported Neuropixels 2.0 with 5120 recording sites distributed over four shanks in 2021 [48]. To improve the mechanical match between probe and tissue, flexible probes have gradually become a research hotspot. Musk and his company Neuralink [32] proposed high-density flexible probes with 3072 electrode sites per array distributed across 96 threads, 4–6-μm-thick and approximately 20-mm length, which can be inserted by a neurosurgical robot with micron precision (Figure 2(f)). Additionally, multifunctional probes have drawn a lot of attention, enabling researchers to measure electrophysiological or chemical signals and synchronously influence subject behaviors. Cai et al. [65] proposed a silicon probe array with platinum nanoparticles and reduced graphene oxide nanocomposites (Pt/rGO) modification for simultaneous real-time monitoring of dopamine (DA) concentration and neural spike firings under deep brain electrical stimulation.

## 3 Processing chips, controllers, and basic circuits

Signal processing chips, controllers, and other basic circuits are essential components for the construction of a complete wireless epicortical or intracortical neuronal recording system. They are also the key to guaranteeing the high fidelity of neural signals and subsequent real-time transmission.

First, from the perspective of the signal-flow sequence, signal processing chips include analog signal amplifiers, filters, multiplexers, and analog-to-digital converters (ADC) [18]. The electrical signal recorded by an electrode is usually at a level from μV to mV. The weak signal makes it difficult to carry out subsequent processing and is easily drowned in noise. Therefore, an amplifier is required to amplify the signal to a higher voltage range that is easier to process. The function of the filter is to filter out high-frequency noise and the power frequency signal and to improve the signal-to-noise ratio. In fact,



the signal of each channel needs to be amplified and filtered. Therefore, a large number of channels in the system will lead to redundancy of the subsequent signal processing circuit and an increase in energy consumption and equipment volume.

To address this issue, a multiplexer is employed to enable multiple signal recording channels to be processed by one channel in a multiplexed method (e.g., 8:1, 16:1). At this point, the recorded signal is analog, and the next steps of signal processing and wireless data transmission are carried out in the form of digital signals; therefore, the signal should be converted to digital by an ADC. An analog signal is a signal whose mathematical form is a continuous function in the time domain. Most signals in nature are analog signals, such as EEG (electroencephalogram)/ECoG/spike signals and electromagnetic signals. Digital signals are discrete signals in the time domain and in amplitude, which can easily carry out logic or arithmetic operation through the processor and be stored in a medium. Analog processing methods mainly include amplification, filtering, multiplexing, and signal conversion. The relevant processing chips include power management, amplifier, filter, and signal conversion chips. As a comparison, digital processing methods are mainly logic and arithmetic operations, with processing chips such as a central processing unit (CPU), system on chip (SoC), microcontroller unit (MCU), and field-programmable gate array (FPGA).

Second, as the brain of the whole system, the controller is responsible for configuring the parameters of each module, collecting digital signals transmitted by the ADC, and controlling the radio circuit for wireless data transmission. In addition, some systems may integrate temperature sensors, an inertial measurement unit. The information from these sensors will be transmitted to a radio circuit or analyzed by the controller.

Lastly, in order to keep the whole system functioning, basic circuits are also nonnegligible, such as the power management unit (PMU), which provides a stable power supply to the system and ensures circuit safety during charging, and the radio SoC, which conducts wireless transmission according to specific protocols. The scheme of wireless transmission and power supply will be described in Sections 4 and 5.

Each of the units described above is generic and different wireless neural signal recording systems have similar and corresponding functions. They could be divided into four schemes according to the degree of system integration: (1) modular distributed [19, 67–70], (2) stacked [24, 26, 71, 72], (3) integrated [32, 73–79], and (4) ultracompact [80–84]. In addition, there are differences in miniaturization, lightweight, and functional expansion between different schemes, which will be described in detail below.

### 3.1 Modular distributed scheme

This type of system usually uses a large number of commercial off-the-shelf (COTS) modules, which have the advantage of quickly building a complete system with relatively low prices and little time. For example, amplifier chips from the Intan company are used as front-end chips for signal amplification, filtering, and analog-digital conversion [27, 70, 71, 85]. ARM (Advanced RISC Machines) cortex architecture core chips are used as controllers [18, 19, 22, 68]. Commercial radio chips are used as wireless transmission circuits, and commercial FPGAs are used as digital signal processing chips [19, 22, 67, 71]. As shown in Figure 3(a), the modular distributed scheme is typical [68]. The PennBMBI neural signal analyzer (NSA) has both neuronal signal recording and analysis capabilities. NSA consists of an analog front-end, microcontroller, power management module, commercial wireless transceiver module, and MicroSD card. Its analog front-end has four channels, each containing two-stage amplifier circuits. The total gain of the system can be set from 46 to 102 dB. NSA uses a 32-bit MCU (AT32UC3C1512C, Atmel company) that integrates a 12-bit resolution ADC, multiplexer, sample hold (S/H) circuit, programmable amplifier, and a 32-bit floating-point arithmetic digital signal processor (DSP) unit. NSA can process neural signals online through DSP units. The volume of the system is 56 mm×36 mm×13 mm.

### 3.2 Stacked scheme

Building a modular distributed system with COTS components reduces the cycle and cost of system development but simultaneously brings the problem of a large area of the printed circuit board (PCB), making it difficult to miniaturize the system. To address this issue, some researchers have proposed a method of dividing the PCB board into modules, connecting the modules with flexible flat cable, then folding to reduce the area of PCB [22, 71]. The 3D stack method is a representative method for reducing system size [24, 26, 72, 86]. Figure 3(b) shows a typical stacked system consisting of the front-end chip (RHD2132, Intan Technologies), FPGA (Spartan-6, Xilinx company), radio chip (nRF24L01, Nordic

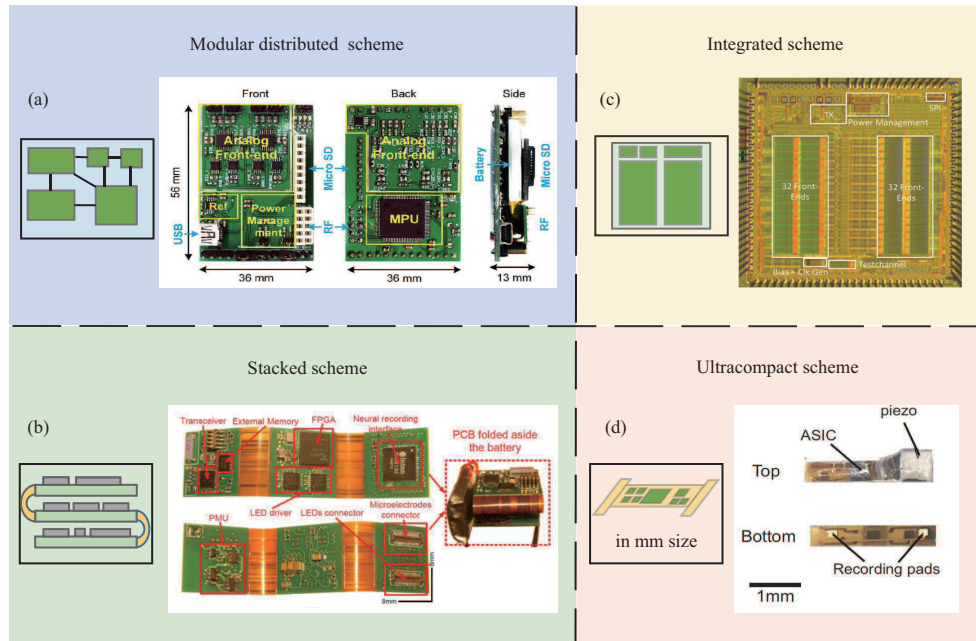


**Figure 3** (Color online) Different composition schemes of a signal processing chip, controller, and basic circuit. (a) Modular distributed scheme using a large number of COTS [68] Copyright 2015 IEEE; (b) stacked scheme in which units are connected by flexible cables [71] Copyright 2017 IEEE; (c) typical custom application-specific integrated circuit scheme manufactured by a CMOS process [73] Copyright 2014 IEEE; (d) ultracompact system with a volume of  $2.4 \text{ mm}^3$  [82] Copyright 2016 Elsevier.

Semiconductor), PMU, and external memory [71]. All components are divided into three parts and placed on a rigid-flex PCB. The three parts are connected by two flexible PCBs.

### 3.3 Integrated scheme

The stacked scheme reduces the size of the system to some extent, but it is not sufficient to realize miniaturization and light weight, and modular systems often cannot meet the demand of a large number of channels. In recent years, researchers have made great progress in miniaturization, high channel count, and low power consumption using CMOS processing technology [32, 73–79]. Table 2 [16, 23, 71, 72, 74, 77, 83, 87, 88] compares recent chips for implantable BCI using COMS technology. Although the latest CMOS process level can reach 7 nm, the signal preprocessing chip is an analog application-specific integrated circuit (ASIC) for BCI, which places more emphasis on the quality of signal processing, such as precision, reliability, and stability. The analog ASIC has a higher operating current than the digital ASIC; thus, the CMOS process for a 5-nm CPU cannot be used directly for preprocessing chips. However, a digital chip that carries on the processing to the digital signals mainly focuses on the computation ability, which needs more logic gates and arithmetic units, as well as a higher main frequency. Thus, the use of more advanced processes is preferred whenever possible. In general, advanced processes can be of great help in facing the challenges of high throughput, low power consumption, and miniaturization in wireless neuronal recording systems. Elon Musk’s Neuralink company has developed a system consisting of a custom ASIC, which integrates multiple ASICs on a PCB using a flip-chip integration to achieve 3072 channels for signal recording. As shown in Figure 3(c), this is part of an integrated system that is manufactured using 65-nm CMOS technology (from STMicroelectronics) [73]. This chip integrates a 64-channel front-end, ADC, PMU, wireless transmission unit, bias circuitry, clock, and serial peripheral interface (SPI). The total area of the chip is  $2.4 \text{ mm} \times 2.4 \text{ mm}$  with a power consumption of  $225 \mu\text{W}$ . Such systems are usually customized for specific functions and integrate a variety of necessary functions on a small chip. It greatly reduces the size and power consumption of the system and is more conducive to implantation and wireless power supply.

### 3.4 Ultracompact scheme

Custom integrated systems manufactured using CMOS technology make it possible for a system to realize a light weight and low power consumption. But some system components, such as antenna and electrode

**Table 2** Comparison of different chips for implantable BCI using COMS technology

Ref.	Process (nm)	Area (mm <sup>2</sup> )	Power supply (V)	Power (μW/ch)	CMRR (dB)	PSRR(dB)
[16]	500	25.48	3	60	>60	>50
[87]	65	0.04	0.35/0.7	0.37	78	110
[71]	65	1.6	0.5	2.3	88	67
[72]	180	2.56	–	79	>83	–
[77]	350	1.1	1.8	<300	–	–
[23]	130	12	1	11.7	–	41
[83]	130	12.19	1.2	12–98	–	–
[88]	180	5	1.2	1.875	–	–
[74]	350	0.115	3.3	Total 24.75	>70	>66

pads, tend to be larger in size. As shown in Figure 3(d), researchers have proposed a “Neuro dust” scheme [80–84], a millimeter-scale system consisting of a pair of gold recording pads (0.2 mm×0.2 mm), a custom single transistor, and a piezoelectric crystal [82]. The piezocrystal, which is impacted by ultrasound pulses, converts the ultrasonic energy into electrical energy to supply power to the system. Therefore, the neural dust does not need a built-in battery or a larger coil, and its total volume is only 2.4 mm<sup>3</sup>. In summary, the ultracompact scheme has fewer channels but can be used for high spatial resolution and independent recording of multiple discrete points through multiple systems. It also has greater advantages in miniaturization. In brief, it provides a new solution for building wireless neural recording systems.

### 3.5 Some commercial products

Several commercial corporations have been working on wireless implants in recent years, mainly because of the integration of high-performance chips, and are welcomed by a fast-growing number of users. Blackrock Microsystems has launched the two latest wireless recording systems, the CerePlex Exilis and CerePlex W. CerePlex Exilis supports 32/64/96 channels, 30 kSps sampling frequency, and 16-bit resolution during signal acquisition. The input signal frequency range is 0.3 Hz to 7.5 kHz, the equivalent input noise is less than 3 μVrms, the subject animals can freely move within a 1-m range, and the maximum continuous operating time is 2.5 h while powered by a battery. In comparison, the CerePlex W has the same sampling frequency, resolution, input signal frequency range, and equivalent input noise but uses the Honey Badger ASIC Chip for longer continuous operation, up to 3.5 h, and a larger maximum free movement range of 2 m. The CerePlex Exilis (9.87 g) is lighter than the CerePlex W (33.5 g). Compared with current academic results, the main advantages of Blackrock’s products are their good recorded-signal quality, higher sampling frequency, resolution, accuracy, and transmission rate. On the other hand, their disadvantages are higher power consumption and shorter continuous operation time without a wireless power supply.

The Plexon DataLogger wireless data recording system can support 32-channel signal acquisition with a 40-kHz sampling rate and 16-bit sampling resolution. However, it does not support real-time neural signal data transmission, which means the data needs to be downloaded after recording. The continuous operation time is also short (up to 45 min).

Bio-signal technologies has also proposed a wireless electrophysiological recording system, Eros, which can support 4/8 channels, 250-Hz sampling frequency, 24-bit sampling accuracy, 4–6 h battery life, and a 10-m working distance. Compared with other products, it has fewer channels and a lower sampling frequency.

## 4 Wireless data transmission

Compared with the wired system, a significant difficulty to cope with is the elimination of cables for wireless communication, which includes uplink and downlink communications [89]. The uplink communication can transmit digitalized neural data to an external base station for status monitoring and further analysis. Inevitably, acquired data from hundreds of recording electrodes can quickly come to hundreds of megabits per second (Mbps), so uplink communication requires a higher data transmission rate. At the same time, this leads to higher power dissipation. In comparison, downlink data communication from the external station to the neuronal recording system results in much lower power dissipation, at



**Table 3** Comparison of different wireless data transmission schemes

Ref.	Number of channels	Wireless data transfer type	Data rate	Transmission distance	Wireless transmission power consumption	Year
[92]	46	Infrared light 880–900 nm	4 Mbps	–	–	2012
[16, 26]	100	FSK 3.2–3.8 GHz	24 Mbps	>1 m	50 mW	2013
[93]	100	UWB 3.1–5 GHz	200 Mbps	1–2 m	–	2014
[94]	64	UHF MICS band 402–405 MHz	450 kbps	2 m	19.8 mW	2015
[86]	64	2.4 GHz with 802.11 b/g/n protocol	1.536 Mbps	2 m	–	2016
[18]	128	2.4 GHz BLE	1.96 Mbps	2 m	11.8 mA (+4 dBm)	2019
[24]	8/36/72	RF 2.4 GHz	2 Mbps	Max 50 m	–	2020

both the transmitter and receiver sides, because it only needs to transmit configuration information and control instructions, such as the active number of electrodes and the sampling rate of the ADC. The ECoG signal frequency is less than 200 Hz for the human brain, the spikes are in the range of 0.1–7 kHz, and the LFP is also smaller than 200 Hz [90]. According to the Nyquist-Shannon sampling theorem [91], when a signal with frequency  $f$  is sampled, the sampling frequency must ideally be no less than  $2f$  to restore the sampled signal without distortion. Therefore, the sampling frequency of AD conversion for epicortical ECoG signals ( $\sim 1$  kHz) is much lower than that for intracortical spikes ( $\sim 20$  kHz), which results in different requirements for wireless data transmission and rate. In simple terms, ECoG signals of 100 channels are recorded with an ADC for analog-to-digital conversion. The sampling frequency is 1 kSps and the resolution is 12-bit. The size of the serial data stream generated is  $100 \text{ ch} \times 1000 \text{ Sps/ch} \times 12 \text{ bit/S} = 1.2 \text{ Mbps}$ . Therefore, the wireless transmission rate should be at least greater than 1.2 Mbps. This calculation method is also suitable for the transmission rates of spikes.

Typical wireless data transmission schemes from the last decade are compared by channel count, wireless data transfer type, data rate, transmission distance, and wireless transmission power consumption in Table 3 [16, 18, 24, 26, 86, 92–94].

According to the different physical forms, the wireless transmission mode adopted by a wireless neuronal recording system can be divided into RF [26, 67, 68, 73, 85, 94, 95], infrared (IR) [26, 92, 96], and ultrasonic communication [79]. RF communication has been widely used because of the little influence of occlusion and the difficulty of technical implementation. With the development of RF communication technology, it is easy for signal crosstalk to occur when using the same frequency band for communication. Therefore, organizations and technical alliances such as IEEE made a division of the frequency band. Electronic devices for short-range wireless communication usually work in the industrial scientific medical (ISM) band. In addition, some standard communication protocols, such as Bluetooth [23, 31, 70], WiFi [19, 86, 97], and ZigBee [17], have been gradually developed. These standard protocols set strict specifications at the physical and link layers, so the cost and technical difficulty of implementation are low, and COTS components can be easily used. In 2019, Zhou et al. [18] used 2.4-GHz low-power Bluetooth technology to achieve wireless communication of the intracortical LFP recording system and base station in non-human primates (Figure 4(a)). The commercial Bluetooth Radio SoC (nRF51822, Nordic Semiconductor) was used for the customization of Bluetooth protocol to achieve a 2 Mbps modulation rate within a 2-m distance.

However, because Bluetooth and WiFi are widely used in electronic devices, they are very prone to signal interference when applied to implantable medical devices. Customized wireless communication technology can effectively avoid this problem. In 2014, Mestais et al. [94] realized wireless data communication between an epicortical ECoG recording system and PC using ultrahigh-frequency (UHF) transmission technology in non-human primates (Figure 4(b)). The UHF link works in the medical implant communication service (MICS) band using a custom protocol in the 400 MHz range. The low-level communication protocol is realized by a radio chip (ZL70102, MicroSemi company) with an energy per bit of less than 21 nJ and a maximum payload throughput of up to 500 kbps. Finally, a transmission rate of up to 450 kbps is achieved by a custom platinum antenna at a maximum distance of 2 m.

The use of infrared communication can also reduce interference between different devices. In 2009, Song et al. [96] adopted RF function multiplexing technology in a 16-channel broadband spike recording

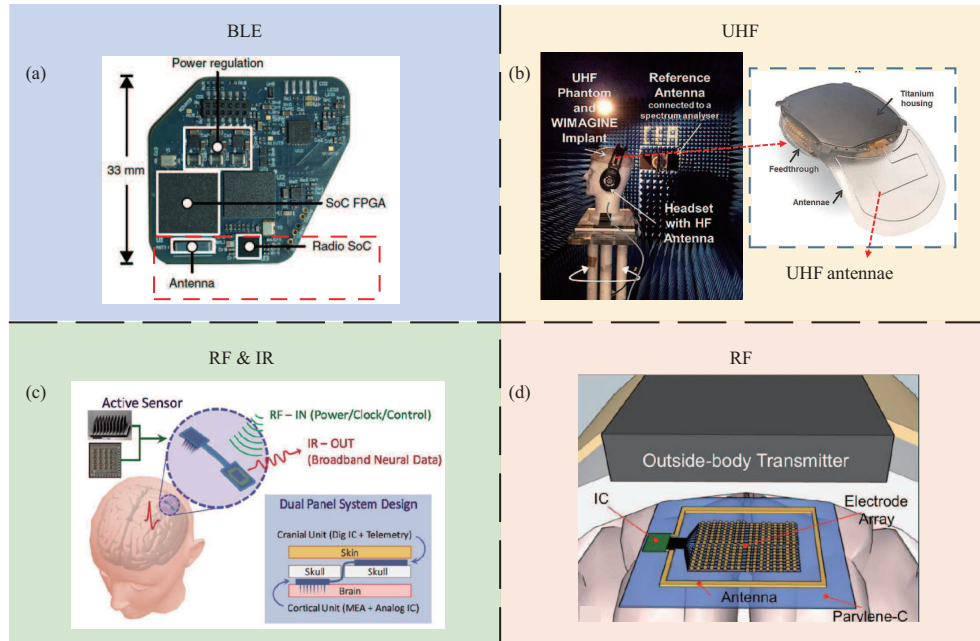


**Figure 4** (Color online) Different wireless data transmission methods. (a) Bluetooth low energy (BLE) communication with radio SoC and a custom antenna [18] Copyright 2019 Springer Nature; (b) UHF radio frequency communication operating in the MICS band [94] Copyright 2014 IEEE; (c) RF transmission function multiplexing and IR transmission [96] Copyright 2009 IEEE; (d) RF for simultaneous power supply and data transmission [73] Copyright 2014 IEEE.

system in a nonhuman primate (Figure 4(c)). The 13.56-MHz RF signal is sent to a gold spiral on the back of the epicranial section to supply power to the system. At the same time, the controller modulates the signal to obtain clock signals and control instruction information. The controller converts the multi-channel neural signal data into the driving current, drives the IR signal of a specific frequency, and transmits data to the outside.

In addition, backscattering modulator technology can simultaneously carry out wireless communication and supply power, avoiding the use of two antennas or coils, respectively, reducing the volume and power consumption of the system. In 2014, Muller et al. [73] used backscattering modulator technology to transmit serialized data at a rate of 1 Mbps. In this way, a single antenna can simultaneously power and transmit data wirelessly to the system (Figure 4(d)).

In fact, modulation technology is the key to realizing wireless communication. To put it simply, the function of modulation is to convert low-frequency baseband signals containing information into high-frequency carrier signals. By modulating to different frequencies, interference of different signals can be effectively avoided in communication. Modulation can be divided into analog modulation and digital modulation according to different modulation signals. Compared with analog modulation, digital modulation has stronger anti-interference capability and confidentiality and is convenient for device integration and signal processing by computer. Digital modulation can be divided into amplitude shift keying (ASK), phase shift keying (PSK), and frequency shift keying (FSK) according to the different high-frequency carrier parameters of digital signals. ASK is more widely used due to its technical difficulty and low energy consumption. For binary ASK modulation technology, the digital signal “1” sends a carrier signal with a larger amplitude, and “0” sends a carrier signal with a smaller amplitude. When the digital signal is “0”, no carrier signal is sent so as to further reduce energy consumption, which is the simplified ASK modulation technology, and is known as on-off keying (OOK) modulation technology [98]. Therefore, OOK modulation technology is very suitable for the wireless communication signal modulation of low power electronic devices. In 2014, Yin et al. [93] adopted OOK modulation technology to achieve a maximum transmission rate of 200 Mbps with low power consumption and a DC/RF conversion efficiency of 40%.

## 5 Power supply

Wired systems are generally powered by cables without energy shortage, but the power supply is a significant challenge for continuous monitoring wireless systems. A large number of electrodes, amplification,

**Table 4** Comparison of different wireless power transmission schemes

Ref.	Power supply mode	Power consumption	Running time	Year
[26]	200 mAh battery with 2 MHz wireless charging	90.6 mW	7 h	2013
[93]	1.2 Ah 3.6 V disposable battery	17 mA(low-RF) or 27 mA(high-RF)	48 h	2014
[94]	13.5 MHz inductive link	75 mW (32 ch@1 kHz, w/o charging) 350 mW w/ charging	Unlimited	2015
[73]	300 MHz RF Power	2.3 $\mu$ W/ch total:225 $\mu$ W	Unlimited	2015
[85]	Rechargeable 3.7 V battery with ultrasonic charging	4.22–15.4 mA	–	2016
[22]	1.6 Wh battery with 265 kHz magnetic resonance coupling	200 mW(w/o charging) 400 mW(w/ charging)	8 h	2018
[18]	500 mAh Lithium-ion battery	172 mW	11.3 h	2019
[99]	30 mAh 3.7 V rechargeable battery	28.6 mW	2.5 h	2021

digitalization, and wireless transmission lead to great energy needs [89]. There are several methods to power up wireless systems. Power consumption and running times of typical wireless power transmission schemes are compared in power supply mode in Table 4 [18, 22, 26, 73, 85, 93, 94, 99].

### 5.1 Battery

The traditional solution is to use built-in batteries to power the system, as in pacemakers and cochlear implants [93, 98–100]. Batteries have been used in medical applications since 1973 [101]. Figure 5(a) demonstrates a battery-powered solution. In 2014, Yin et al. [93] used a disposable AA Li-ion battery (1.2 Ah, Saft Groupe S.A.) to power a system. The system integrates three customized low-power ASICs so the battery can sustain power for more than 48 h.

### 5.2 Wireless charging

A battery has a limited life and needs to be replaced when the power runs out. Therefore, such a system cannot be fully implanted or requires battery replacement by surgery, which often causes unnecessary damage to biological tissue. To avoid the biological impact of battery replacement, some researchers have proposed charging batteries wirelessly [22, 26, 72, 85, 102]. Figure 5(b) shows a typical wireless charging scheme for a built-in battery. In 2018, Matsushita et al. [22] proposed a wireless neuronal recording system, named W-HERBS, that uses a lithium-ion polymer rechargeable battery as the power supply. Meanwhile, the magnetic resonance coupling method is used to charge the battery, avoiding the need for battery replacement. During wireless charging, the external transmitter unit uses the 265-kHz magnetic frequency to carry out magnetic coupling with the receiver unit. It can transmit 400 mW of electrical energy, meeting the energy consumption of the system (200 mW) and battery charging (200 mW) at the same time.

### 5.3 Wireless power supply

The battery power scheme solves the power supply problem for wireless systems, but batteries often occupy a large proportion of the volume and weight, which hinder the miniaturization and light weight of a system. Meanwhile, a battery risks electrolyte leakage, which may cause serious harm to organisms during implantation. Fortunately, a wireless power supply is a good solution to the above issues. According to different forms of energy transfer, wireless power supply schemes can be divided into two types: electromagnetic energy transfer [67, 73, 92, 94–96, 103] and other energy transfer forms, such as infrared [104] and ultrasound [82]. Figure 5(c) illustrates a wireless charging scheme based on inductive coupling, which was proposed by Mestais et al. [94] in 2014. The system obtains 100 mW of power from the external antenna through the 13.56-MHz induction link. It is sufficient to supply the system with an overall energy consumption of 75 mW.

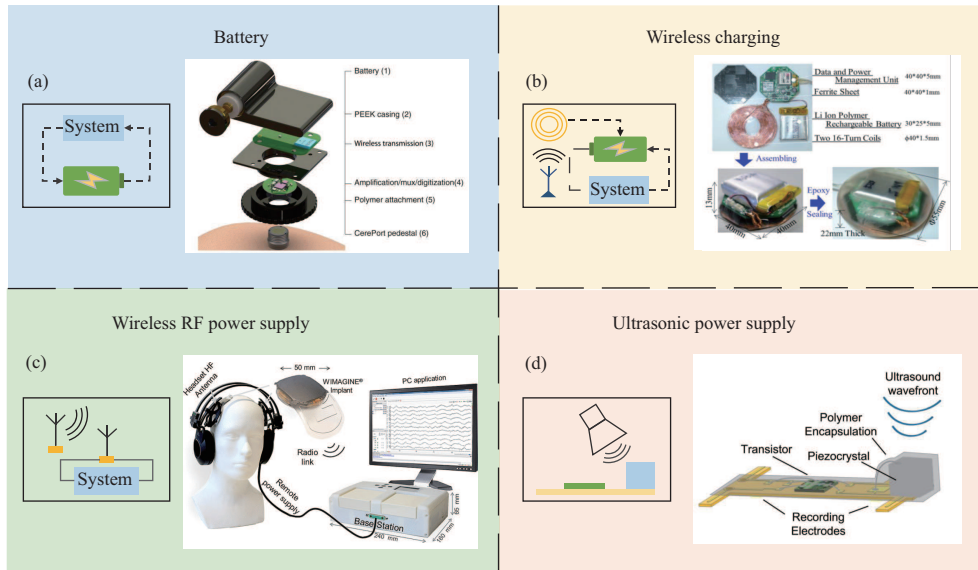


**Figure 5** (Color online) Different power supply modes. (a) Powered directly by disposable or rechargeable battery [93] Copyright 2014 Elsevier; (b) powered by rechargeable battery with wireless charging (CC BY) [22] Copyright 2018 Matsushita et al.; (c) wireless power supply by RF [94] Copyright 2014 IEEE; (d) wireless power supply by ultrasound [82] Copyright 2016 Elsevier.

The influence of a wireless power supply on signal recording cannot be ignored. On the one hand, the use of near-field magnetic coupling or an RF wireless power supply with RF wireless communication will cause interference of communication signals and affect the quality of transmitted signals. On the other hand, electromagnetic induction can also induce current on the metal electrodes, which can affect the quality of the original neural signals to a certain extent. For the first issue, some researchers have tried to use different working frequency bands. For example, the power supply frequency of magnetic resonance coupling is set to 265 kHz, and the RF wireless communication frequency is set to 2.4 GHz [22]. Another work sets the high-frequency wireless power supply frequency to 13.56 MHz, the RF wireless communication frequency to 402–405 MHz as the MICS band, and a filter is added to filter out the electromagnetic wave of the corresponding frequency [94]. For the second issue, not only the signals of wireless power supply but also the signals of wireless communication and environmental noise will affect the original neural signals. Therefore, researchers usually filter out interfering signals during signal pretreatment or reduce the influence on signal detection by adding metal shells [16]. In addition, other forms of energy conversion, such as photovoltaic or ultrasonic wireless power supply, may be applied to solve this problem.

Meanwhile, compared with near-field (NF) coupling, far-field (FF) radiation, or RF transmission, ultrasound (US) is a superior method for powering a recording system for deeper implantation. US utilizes sound waves as the carrier of energy. Figure 5(d) shows a charging scheme of the neural dust mentioned above [82]. The external transducer sends US pulses to a piezoelectric crystal, which converts the mechanical energy of the US pulse into electrical energy to supply power to the system.

In general, a battery can provide more power than a wireless power supply because high-power wireless charging must consider heat generation and the electromagnetic intensity range acceptable to the human body. Therefore, the power supply scheme selected needs to be comprehensively considered among system power consumption, channel number, signal quality, wireless transmission scheme, and total system volume.

## 6 Package

The above sections have summarized approaches to wireless neuronal recording systems from electrodes, chips, data transmission to the power supply. At this point, the system is fully operational, but the packaging of the system is nonnegligible to guarantee its life-lasting stability *in vivo*. There are two main considerations in packaging. First, the system should meet strict requirements of water vapor tract ratio (WVTR) and oxygen tract ratio (OTR) to avoid a short circuit via a good water and gas barrier [105–109].

Second, the packaging housing should employ biocompatible materials to prevent rejection by biological tissue [110–113]. In 2012, Schuettler et al. [92] proposed a wireless epicortical neuronal recording system named BrainCon using alumina ceramic as the hermetic package material to protect the core chips and circuits from water-induced corrosion, as shown in Figure 6(a). Meanwhile, polydimethylsiloxane (PDMS) and Parylene-C (optionally) were coated on the outside packaging. The package not only passed the gross leak test, but fine leak tests on a mass-spectrometer based leakage tester (SmartTest HLT570, Pfeiffer Vacuum, Asslar, Germany) also proved good hermeticity. Practically, the package works well in animal experiments lasting for about one year. In 2014, Mestais et al. [94] reported another wireless epicortical neuronal recording system with 64 channels named WIMAGINE, which used dedicated titanium packaging with customized hermetic feedthroughs to guarantee all electronics were in hermetic housing, as pictured in Figure 6(b). The hermetic feedthroughs are based on a ruby insulator, with additional gold brazing for hermeticity. All components were tested individually by helium leakage testing with  $10^{-9}$  bar·cm<sup>3</sup>·s<sup>-1</sup>. Additionally, thermally conductive silicone pads were laid between the top electronic PCB and titanium housing to avoid biological tissue damage by system heat. Moreover, the PCB stacking is optimized using conductive glue and heat sinks to further weaken the thermal impact. Finally, the overall size of WIMAGINE is 50 mm in diameter and 12.54 mm in height with a 10 cm<sup>2</sup> HF Antenna and was implanted in nonhuman primates for ECoG recording, which lasted for 26 weeks with good biocompatibility.

When infrared signals are used for communication, the transparency of the system housing should be enhanced to reduce signal loss. When applying RF technology for communication or power supply, it is also necessary to avoid energy loss caused by metal housing and the impact of induced current on organism safety. In 2013, Yin et al. proposed a wireless intracortical neuronal recording system linked to a Utah array with sealing and packaging by laser welding of two titanium metal cases (56 mm×42 mm×9 mm, 30.6 g) [16,26], as shown in Figure 6(c). They assembled a single-crystal sapphire window with a diameter of 29.2 mm by copper welding, achieving 93% IR transparency at a 5-mm distance from the window and <50% RF loss for the radio transmitter. In 2019, Musk and his company Neuralink [32] released an intracortical neuronal recording system linked to flexible probes and packaged in titanium cases, as pictured in Figure 6(d). It was coated with Parylene-C as a moisture barrier to prevent fluid inflow and prolong its lifetime. Two configurations of the recording system have been proposed, with 1536 and 3072 channels, and their corresponding volumes and weights are 24.5 mm×20 mm×1.65 mm and 11 g and 23 mm×18.5 mm×2 mm and 15 g, respectively. They upgraded this system to LINK V0.9 in August 2020, a coin-size wireless charging version with 1024 recording channels, all-day battery life, and a size of 23 mm×8 mm [114].

## 7 Conclusion and challenges

This review summarizes the latest development in wireless implantable neuronal acquisition systems, including high-density neural recording electrodes, dedicated low-power ASICs, wireless data transmission modes, wireless power supply modes, and highly reliable hermetic packages. The above units in the BCI are important factors that determine communication efficiency and human-computer interaction ability. The system-level wireless neuronal acquisition will surely become one of the most important development trends in the future and will get rid of wired constraints and enhance independence and mobility for human use.

The human brain has more than 80 billion neurons; however, current systems are far from sufficient to handle such a large number. The development of wireless implantable neuronal recording systems still faces many challenges as described below.

**(1) High throughput.** At the World Artificial Intelligence Conference 2021, Tiger H. Tao and colleagues from Shanghai Microsystems Research Institute, China, released their latest work on high-throughput, minimally-invasive, flexible probes with 2640 channels on a single device. Compared with the increase of the number of electrodes, the greater challenges are how to firmly connect the electrodes to the circuit when the number of electrodes reaches more than 10000, how to carry out high-fidelity amplification, filtering, and analog-to-digital conversion of neural signals with high channel count, and how to process high-throughput data algorithmically. In addition, consequent problems with wireless transmission, power supply, and heat also need to be synthetically solved.

**(2) Wireless transmission.** For a wired recording system, the Argo with 65536 channels produces



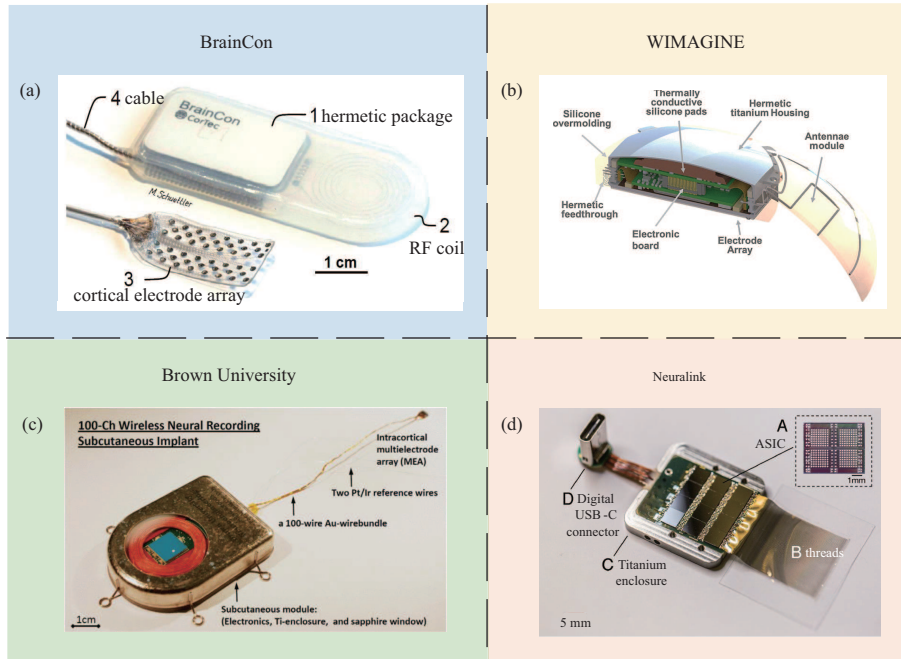


**Figure 6** (Color online) Representative system-level packages for neuronal recording. (a) BrainCon: wireless epicortical neuronal recording system packaged by alumina ceramic and coated with PDMS and Parylene-C [92] Copyright 2012 IEEE; (b) WIMAGINE: wireless epicortical neuronal recording system packaged by hermetic titanium housing [94] Copyright 2014 IEEE; (c) wireless intracortical neuronal recording system packaged by titanium cases (lid removed) and coated with Parylene-C [16] Copyright 2013 IEEE; (d) wireless intracortical neuronal recording system packaged by titanium casing with single-crystal sapphire window (CC BY-ND 4.0) [32] Copyright 2019 Elon Musk, Neuralink.

a readout data rate of up to 26 Gbps, as previously introduced. In comparison, the wireless recording system (LINK V0.9) by Neuralink can only support the wireless transmission of compressed data at a spike firing by Bluetooth. Therefore, wireless transmission of high-throughput data remains a major challenge since commonly used RF technologies are often limited by power consumption and heat dissipation.

**(3) Power consumption and supply.** Power budgets often limit the number of recording channels because signal processing and wireless data transmission consume large amounts of power. At the same time, the heat from electromagnetic induction also limits the power of wireless energy transmission. Taking Neuralink’s 3072 channel wired recording system as an example, its system power consumption is 750 mW, and its latest wireless 1024 channel LINK V0.9 can work all day with a battery life of 24 h (wireless charging) and with much lower power consumption at the expense of the complete waveform of spikes. As for the power supply, the 128-channel W-HERBS system can reach a maximum charging power of 400 mW, as mentioned earlier. However, for wireless recording systems with more than 10000 channels, the wireless charging power is far from sufficient under the premise of biosecurity.

**(4) Heat accumulation.** Due to full implantation in the intracranial space, a packaged system needs to consider heat-induced temperature rise, which may lead to thermal damage to the brain tissue. According to the ISO 14708-1:2000 E standard, the temperature rise should be constrained to 2°C on the external surface of the implanted device. Therefore, heating limits the wireless transmission rate and power of the system. As previously mentioned, thermally conductive silicone pads, conductive glue, heat sinks, and titanium housing are used in the WIMAGINE system for optimized thermal management. Nevertheless, heat dissipation technology needs further development for wireless recording systems with high-throughput wireless transmission and high-power supply.

**(5) Minimization.** Components such as electrode pads, processing and computing circuits, wireless power supply coils, wireless data transmission antennas, built-in batteries, and heat dissipation units limit the overall size of the system to be smaller. As mentioned earlier, the overall size of Neuralink’s LINK V0.9 has been limited to 23 mm×8 mm as a highly integrated solution. In the future, the miniaturization of a wireless recording system with more than 10000 channels needs further development in regard to structure optimization and highly integrated system components.

**(6) Lifetime.** Until now, the longest implantation lifetime of a wired Utah array recording system ranged from six (BrainGate project) to nine years (Nicho Natsopoulos, University of Chicago) for non-

human primates. Meanwhile, these systems have a lifespan of up to seven years for humans. However, the lifetime of existing wireless neuronal recording systems is affected by many factors, and their reliability for chronic implantation life has been insufficiently verified.

Overall, the wireless implantable neuronal recording system is an emerging research field with strong comprehensiveness and interdisciplinary integration. It involves micro-nano manufacturing, microelectronics, communication, energy, biomedicine, brain science, and artificial intelligence. With the development of the above technologies, wireless implantable BCI systems will become more miniaturized, integrated, and intelligent for broader applications in humans in the next decade.

**Acknowledgements** This work was supported by China Postdoctoral Science Foundation (Grant Nos. 2020TQ0246, 2021M692-638), Shanghai Sailing Program (Grant No. 21YF1451000), Fundamental Research Funds for the Central Universities (Grant No. 31020200QD013), and Natural Science Foundation of Chongqing (Grant No. cstc2021jcyj-msxmX0825).

## References

- 1 Homer M L, Nurmikko A V, Donoghue J P, et al. Sensors and decoding for intracortical brain computer interfaces. *Annu Rev Biomed Eng*, 2013, 15: 383–405
- 2 Brandman D M, Cash S S, Hochberg L R. Human intracortical recording and neural decoding for brain-computer interfaces. *IEEE Trans Neural Syst Rehabil Eng*, 2017, 25: 1687–1696
- 3 Szostak K M, Grand L, Constandinou T G. Neural interfaces for intracortical recording: requirements, fabrication methods, and characteristics. *Front Neurosci*, 2017, 11: 665
- 4 Miller K J, Hermes D, Staff N P. The current state of electrocorticography-based brain-computer interfaces. *NeuroSurg Focus*, 2020, 49: 2
- 5 Sharma K, Sharma R. Design considerations for effective neural signal sensing and amplification: a review. *Biomed Phys Eng Express*, 2019, 5: 042001
- 6 Vansteensel M J, Pels E G M, Bleichner M G, et al. Fully implanted brain-computer interface in a locked-in patient with ALS. *N Engl J Med*, 2016, 375: 2060–2066
- 7 Moses D A, Metzger S L, Liu J R, et al. Neuroprosthesis for decoding speech in a paralyzed person with anarthria. *N Engl J Med*, 2021, 385: 217–227
- 8 Hochberg L R, Bacher D, Jarosiewicz B, et al. Reach and grasp by people with tetraplegia using a neurally controlled robotic arm. *Nature*, 2012, 485: 372–375
- 9 Flesher S N, Downey J E, Weiss J M, et al. A brain-computer interface that evokes tactile sensations improves robotic arm control. *Science*, 2021, 372: 831–836
- 10 Rajangam S, Tseng P H, Yin A, et al. Wireless cortical brain-machine interface for whole-body navigation in primates. *Sci Rep-Uk*, 2016, 6: 1–13
- 11 Libedinsky C, So R, Xu Z M, et al. Independent mobility achieved through a wireless brain-machine interface. *PLoS ONE*, 2016, 11: 0165773
- 12 Benabid A L, Costecalde T, Eliseyev A, et al. An exoskeleton controlled by an epidural wireless brain-machine interface in a tetraplegic patient: a proof-of-concept demonstration. *Lancet Neurol*, 2019, 18: 1112–1122
- 13 Bouton C E, Shaikhouni A, Annetta N V, et al. Restoring cortical control of functional movement in a human with quadriplegia. *Nature*, 2016, 533: 247–250
- 14 Ganzer P D, Colachis S C, Schwemmer M A, et al. Restoring the sense of touch using a sensorimotor demultiplexing neural interface. *Cell*, 2020, 181: 763–773
- 15 Mahabiz M M, Muller R, Alon E, et al. Reliable next-generation cortical interfaces for chronic brain-machine interfaces and neuroscience. *Proc IEEE*, 2017, 105: 73–82
- 16 Yin M, Borton D A, Aceros J, et al. A 100-channel hermetically sealed implantable device for chronic wireless neurosensing applications. *IEEE Trans Biomed Circ Syst*, 2013, 7: 115–128
- 17 Young C P, Liang S F, Chang D W, et al. A portable wireless online closed-loop seizure controller in freely moving rats. *IEEE Trans Instrum Meas*, 2011, 60: 513–521
- 18 Zhou A, Santacruz S R, Johnson B C, et al. A wireless and artefact-free 128-channel neuromodulation device for closed-loop stimulation and recording in non-human primates. *Nat Biomed Eng*, 2019, 3: 15–26
- 19 Fernandez-Leon J A, Parajuli A, Franklin R, et al. A wireless transmission neural interface system for unconstrained non-human primates. *J Neural Eng*, 2015, 12: 056005
- 20 Wentz C T, Bernstein J G, Monahan P, et al. A wirelessly powered and controlled device for optical neural control of freely-behaving animals. *J Neural Eng*, 2011, 8: 046021
- 21 Chang C W, Chiou J C. A wireless and batteryless microsystem with implantable grid electrode/3-dimensional probe array for ECoG and extracellular neural recording in rats. *Sensors*, 2013, 13: 4624–4639
- 22 Matsushita K, Hirata M, Suzuki T, et al. A fully implantable wireless ECoG 128-channel recording device for human brain-machine interfaces: W-HERBS. *Front Neurosci*, 2018, 12: 511
- 23 Lee B, Jia Y, Mirbozorgi S A, et al. An inductively-powered wireless neural recording and stimulation system for freely-behaving animals. *IEEE Trans Biomed Circ Syst*, 2019, 13: 413–424
- 24 Keramatzadeh K, Kiakojouri A, Nahvi M S, et al. Wireless, miniaturized, semi-implantable electrocorticography microsystem validated in vivo. *Sci Rep-Uk*, 2020, 10: 1–13
- 25 Sauter-Starace F, Ratel D, Cretallaz C, et al. Long-term sheep implantation of WIMAGINE, a wireless 64-channel electrocorticogram recorder. *Front Neurosci*, 2019, 13: 847
- 26 Borton D A, Yin M, Aceros J, et al. An implantable wireless neural interface for recording cortical circuit dynamics in moving primates. *J Neural Eng*, 2013, 10: 026010
- 27 Schwarz D A, Lebedev M A, Hanson T L, et al. Chronic, wireless recordings of large-scale brain activity in freely moving rhesus monkeys. *Nat Methods*, 2014, 11: 670–676
- 28 Simeral J D, Hosman T, Saab J, et al. Home use of a percutaneous wireless intracortical brain-computer interface by individuals with tetraplegia. *IEEE Trans Biomed Eng*, 2021, 68: 2313–2325
- 29 Seo D, Carmena J M, Rabaey J M, et al. Model validation of untethered, ultrasonic neural dust motes for cortical recording. *J Neurosci Methods*, 2015, 244: 114–122

- 30 Park S Y, Kyoungwan N, Voroslakos M, et al. A miniaturized 256-channel neural recording interface with area-efficient hybrid integration of flexible probes and CMOS integrated circuits. *IEEE Tran Bio-Med Eng*, 2021. doi: 10.1109/TBME.2021.3093542
- 31 Liu X L, Zhang M L, Xiong T, et al. A fully integrated wireless compressed sensing neural signal acquisition system for chronic recording and brain machine interface. *IEEE Trans Biomed Circ Syst*, 2016, 10: 874–883
- 32 Musk E. An integrated brain-machine interface platform with thousands of channels. *J Med Int Res*, 2019, 21: 16194
- 33 Willett F R, Avansino D T, Hochberg L R, et al. High-performance brain-to-text communication via handwriting. *Nature*, 2021, 593: 249–254
- 34 Silversmith D B, Abiri R, Hardy N F, et al. Plug-and-play control of a brain-computer interface through neural map stabilization. *Nat Biotechnol*, 2021, 39: 326–335
- 35 Makin J G, Moses D A, Chang E F. Machine translation of cortical activity to text with an encoder-decoder framework. *Nat Neurosci*, 2020, 23: 575–582
- 36 Sung C, Jeon W, Nam K S, et al. Multimaterial and multifunctional neural interfaces: from surface-type and implantable electrodes to fiber-based devices. *J Mater Chem B*, 2020, 8: 6624–6666
- 37 Zhou Y H, Ji B W, Wang M H, et al. Implantable thin film devices as brain-computer interfaces: recent advances in design and fabrication approaches. *Coatings*, 2021, 11: 204
- 38 Ha S, Akinin A, Park J, et al. Silicon-integrated high-density electrocortical interfaces. *Proc IEEE*, 2017, 105: 11–33
- 39 Xing D J, Yeh C I, Shapley R M. Spatial spread of the local field potential and its laminar variation in visual cortex. *J Neurosci*, 2009, 29: 11540–11549
- 40 Buzsáki G, Anastassiou C A, Koch C. The origin of extracellular fields and currents—EEG, ECoG, LFP and spikes. *Nat Rev Neurosci*, 2012, 13: 407–420
- 41 Fallegger F, Schiavone G, Pirondini E, et al. MRI-compatible and conformal electrocorticography grids for translational research. *Adv Sci*, 2021, 8: 2003761
- 42 Renz A F, Lee J, Tybrandt K, et al. Opto-E-Dura: a soft, stretchable ECoG array for multimodal, multiscale neuroscience. *Adv Healthc Mater*, 2020, 9: 2000814
- 43 Kaiju T, Inoue M, Hirata M, et al. High-density mapping of primate digit representations with a 1152-channel  $\mu$ ECoG array. *J Neural Eng*, 2021, 18: 036025
- 44 Shandhi M M H, Negi S. Fabrication of out-of-plane high channel density microelectrode neural array with 3D recording and stimulation capabilities. *J Microelectromech Syst*, 2020, 29: 522–531
- 45 Sahasrabudde K, Khan A A, Singh A P, et al. The Argo: a high channel count recording system for neural recording in vivo. *J Neural Eng*, 2020, 18: 015002
- 46 Kollo M, Racz R, Hanna M E, et al. CHIME: CMOS-hosted in vivo microelectrodes for massively scalable neuronal recordings. *Front Neurosci*, 2020, 14: 834
- 47 Steinmetz N A, Koch C, Harris K D, et al. Challenges and opportunities for large-scale electrophysiology with Neuropixels probes. *Curr Opin Neurobiol*, 2018, 50: 92–100
- 48 Steinmetz N A, Aydin C, Lebedeva A, et al. Neuropixels 2.0: a miniaturized high-density probe for stable, long-term brain recordings. *Science*, 2021, 372: eabf4588
- 49 Guan S, Wang J, Gu X W, et al. Elastocapillary self-assembled neurotassels for stable neural activity recordings. *Sci Adv*, 2019, 5: 2842
- 50 Ji B W, Ge C F, Guo Z J, et al. Flexible and stretchable opto-electric neural interface for low-noise electrocorticogram recordings and neuromodulation in vivo. *Biosens Bioelectron*, 2020, 153: 112009
- 51 Dong R H, Wang L L, Hang C, et al. Printed stretchable liquid metal electrode arrays for in vivo neural recording. *Small*, 2021, 17: 2006612
- 52 Seo J W, Kim K, Seo K W, et al. Artifact-free 2D mapping of neural activity in vivo through transparent gold nanonetwork array. *Adv Funct Mater*, 2020, 30: 2000896
- 53 Qiang Y, Artoni P, Seo K J, et al. Transparent arrays of bilayer-nanomesh microelectrodes for simultaneous electrophysiology and two-photon imaging in the brain. *Sci Adv*, 2018, 4: 0626
- 54 Viventi J, Kim D H, Vigeland L, et al. Flexible, foldable, actively multiplexed, high-density electrode array for mapping brain activity in vivo. *Nat Neurosci*, 2011, 14: 1599–1605
- 55 Schaefer N, Garcia-Cortadella R, Martínez-Aguilar J, et al. Multiplexed neural sensor array of graphene solution-gated field-effect transistors. *2D Mater*, 2020, 7: 025046
- 56 Shi Z F, Zheng F M, Zhou Z T, et al. Silk-enabled conformal multifunctional bioelectronics for investigation of spatiotemporal epileptiform activities and multimodal neural encoding/decoding. *Adv Sci*, 2019, 6: 1801617
- 57 Ji B W, Guo Z J, Wang M H, et al. Flexible polyimide-based hybrid opto-electric neural interface with 16 channels of micro-LEDs and electrodes. *Microsyst Nanoeng*, 2018, 4: 1–11
- 58 Tybrandt K, Khodagholy D, Dielacher B, et al. High-density stretchable electrode grids for chronic neural recording. *Adv Mater*, 2018, 30: 1706520
- 59 Campbell P K, Jones K E, Huber R J, et al. A silicon-based, three-dimensional neural interface: manufacturing processes for an intracortical electrode array. *IEEE Trans Biomed Eng*, 1991, 38: 758–768
- 60 Shobe J L, Claar L D, Parhami S, et al. Brain activity mapping at multiple scales with silicon microprobes containing 1024 electrodes. *J NeuroPhysiol*, 2015, 114: 2043–2052
- 61 Jun J J, Steinmetz N A, Siegle J H, et al. Fully integrated silicon probes for high-density recording of neural activity. *Nature*, 2017, 551: 232–236
- 62 Wei X L, Luan L, Zhao Z T, et al. Nanofabricated ultraflexible electrode arrays for high-density intracortical recording. *Adv Sci*, 2018, 5: 1700625
- 63 Shin H, Son Y, Chae U, et al. Multifunctional multi-shank neural probe for investigating and modulating long-range neural circuits in vivo. *Nat Commun*, 2019, 10: 1–11
- 64 Liu C B, Zhao Y, Cai X, et al. A wireless, implantable optoelectrochemical probe for optogenetic stimulation and dopamine detection. *Microsyst Nanoeng*, 2020, 6: 1–12
- 65 Xiao G H, Song Y L, Zhang Y, et al. Microelectrode arrays modified with nanocomposites for monitoring dopamine and spike firings under deep brain stimulation in rat models of Parkinson's disease. *ACS Sens*, 2019, 4: 1992–2000
- 66 Wang M H, Gu X W, Ji B W, et al. Three-dimensional drivable optrode array for high-resolution neural stimulations and recordings in multiple brain regions. *Biosens Bioelectron*, 2019, 131: 9–16
- 67 Rizk M, Bossetti C A, Jochum T A, et al. A fully implantable 96-channel neural data acquisition system. *J Neural Eng*,

- 2009, 6: 026002
- 68 Liu X L, Zhang M L, Subei B, et al. The PennBMBI: design of a general purpose wireless brain-machine-brain interface system. *IEEE Trans Biomed Circ Syst*, 2015, 9: 248–258
  - 69 Bentler C, Stieglitz T. Building wireless implantable neural interfaces within weeks for neuroscientists. In: *Proceedings of the 39th Engineering in Medicine and Biology Society (EMBC)*, 2017. 1078–1081
  - 70 Kanchwala M A, McCallum G A, Durand D M. A miniature wireless neural recording system for chronic implantation in freely moving animals. In: *Proceedings of IEEE Biomedical Circuits and Systems Conference (BioCAS)*, 2018
  - 71 Gagnon-Turcotte G, Gagnon L L, Bilodeau G, et al. Wireless brain computer interfaces enabling synchronized optogenetics and electrophysiology. In: *Proceedings of IEEE International Symposium on Circuits and Systems (ISCAS)*, 2017
  - 72 Shon A, Chu J U, Jung J, et al. An implantable wireless neural interface system for simultaneous recording and stimulation of peripheral nerve with a single cuff electrode. *Sensors*, 2018, 18: 1
  - 73 Muller R, Le H P, Li W, et al. A minimally invasive 64-channel wireless  $\mu$ ECoG implant. *IEEE J Solid-State Circ*, 2015, 50: 344–359
  - 74 Liu X L, Zhu H J, Zhang M L, et al. A fully integrated wireless sensor-brain interface system to restore finger sensation. In: *Proceedings of IEEE International Symposium on Circuits and Systems (ISCAS)*, 2017
  - 75 Laiwalla F, Lee J, Lee A H, et al. A distributed wireless network of implantable sub-mm cortical microstimulators for brain-computer interfaces. In: *Proceedings of the 41st Annual International Conference of IEEE Engineering in Medicine and Biology Society*, 2019. 6876–6879
  - 76 Lopez C M, Putzeys J, Raducanu B C, et al. A neural probe with up to 966 electrodes and up to 384 configurable channels in 0.13  $\mu$ m SOI CMOS. *IEEE Trans Biomed Circ Syst*, 2017, 11: 510–522
  - 77 Zhang X, Pei W H, Huang B J, et al. A low-noise fully-differential CMOS preamplifier for neural recording applications. *Sci China Inf Sci*, 2012, 55: 441–452
  - 78 Chang S I, Park S Y, Yoon E. Minimally-invasive neural interface for distributed wireless electrocorticogram recording systems. *Sensors*, 2018, 18: 263
  - 79 Liu S Y, Moncion C, Zhang J W, et al. Fully passive flexible wireless neural recorder for the acquisition of neuropotentials from a rat model. *ACS Sens*, 2019, 4: 3175–3185
  - 80 Yeon P, Bakir M S, Ghovanloo M. Towards a 1.1 mm 2 free-floating wireless implantable neural recording SoC. In: *Proceedings of IEEE Custom Integrated Circuits Conference (CICC)*, 2018
  - 81 Kim C, Park J, Ha S, et al. A 3 mm $\times$ 3 mm fully integrated wireless power receiver and neural interface system-on-chip. *IEEE Trans Biomed Circ Syst*, 2019, 13: 1736–1746
  - 82 Seo D, Neely R M, Shen K, et al. Wireless recording in the peripheral nervous system with ultrasonic neural dust. *Neuron*, 2016, 91: 529–539
  - 83 Lee J, Laiwalla F, Jeong J, et al. Wireless power and data link for ensembles of sub-mm scale implantable sensors near 1 GHz. In: *Proceedings of IEEE Biomedical Circuits and Systems Conference (BioCAS)*, 2018
  - 84 Ghanbari M M, Piech D K, Shen K, et al. 17.5 A 0.8 mm 3 ultrasonic implantable wireless neural recording system with linear AM backscattering. In: *Proceedings of IEEE International Solid-State Circuits Conference (ISSCC)*, 2019. 284–286
  - 85 Su Y, Routhu S, Moon K, et al. A wireless 32-channel implantable bidirectional brain machine interface. *Sensors*, 2016, 16: 1582
  - 86 Yoshimoto S, Araki T, Uemura T, et al. Implantable wireless 64-channel system with flexible ECoG electrode and optogenetics probe. In: *Proceedings of IEEE Biomedical Circuits and Systems Conference (BioCAS)*, 2016. 476–479
  - 87 Lyu L, Ye D, Shi C J R. A 340 nW/channel 110 dB PSRR neural recording analog front-end using replica-biasing LNA, level-shifter assisted PGA, and averaged LFP servo loop in 65 nm CMOS. *IEEE Trans Biomed Circ Syst*, 2020, 14: 811–824
  - 88 Jang J W, Kim Y R, Lee C E, et al. A 32ch low power neural recording system with continuously monitoring for ECoG Signal detection. *J Integr Circ Syst*, 2021, 7: 2
  - 89 Türe K, Dehollain C, Maloberti F. *Wireless Power Transfer and Data Communication for Intracranial Neural Recording Applications*. Berlin: Springer, 2020
  - 90 Thakor N V. Translating the brain-machine interface. *Sci Transl Med*, 2013, 5: 210ps17
  - 91 Shannon C E. Communication in the presence of noise. *Proc IEEE*, 1998, 86: 447–457
  - 92 Schuettler M, Kohler F, Ordonez J S, et al. Hermetic electronic packaging of an implantable brain-machine-interface with transcutaneous optical data communication. In: *Proceedings of International Conference on Information Theoretic Security*, 2012. 3886–3889
  - 93 Yin M, Borton D A, Komar J, et al. Wireless neurosensor for full-spectrum electrophysiology recordings during free behavior. *Neuron*, 2014, 84: 1170–1182
  - 94 Mestais C S, Charvet G, Sauter-Starace F, et al. WIMAGINE: wireless 64-channel ECoG recording implant for long term clinical applications. *IEEE Trans Neural Syst Rehabil Eng*, 2015, 23: 10–21
  - 95 Deshmukh A, Brown L, Barbe M F, et al. Fully implantable neural recording and stimulation interfaces: peripheral nerve interface applications. *J Neurosci Method*, 2020, 333: 108562
  - 96 Song Y K, Borton D A, Park S, et al. Active microelectronic neurosensor arrays for implantable brain communication interfaces. *IEEE Trans Neural Syst Rehabil Eng*, 2009, 17: 339–345
  - 97 Xu J, Nguyen A T, Zhao W F, et al. A low-noise, wireless, frequency-shaping neural recorder. *IEEE J Emerg Sel Top Circ Syst*, 2018, 8: 187–200
  - 98 Sharma D K, Mishra A, Saxena R. Analog & digital modulation techniques: an overview. *Int J Comput Sci Commun Technol*, 2010, 3: 2007
  - 99 Idogawa S, Yamashita K, Sanda R, et al. A lightweight, wireless Bluetooth-low-energy neuronal recording system for mice. *Sens Actuat B-Chem*, 2021, 331: 129423
  - 100 Jia Y, Khan W, Lee B, et al. Wireless opto-electro neural interface for experiments with small freely behaving animals. *J Neural Eng*, 2018, 15: 046032
  - 101 Antonioli G, Baggioni F, Consiglio F, et al. Stimulatore cardiaco impiantabile con nuova batteria a stato solido al litio. *Minerva Med*, 1973, 64: 2298–2305
  - 102 Zaeimbashi M, Nasrollahpour M, Khalifa A, et al. Ultra-compact dual-band smart NEMS magnetoelectric antennas for simultaneous wireless energy harvesting and magnetic field sensing. *Nat Commun*, 2021, 12: 1–11
  - 103 Lee B, Koripalli M K, Jia Y, et al. An implantable peripheral nerve recording and stimulation system for experiments on freely moving animal subjects. *Sci Rep-Uk*, 2018, 8: 1–12
  - 104 Moon E, Barrow M, Lim J, et al. Bridging the “last millimeter” gap of brain-machine interfaces via near-infrared wireless

- power transfer and data communications. *ACS Photonics*, 2021, 8: 1430–1438
- 105 Xie X, Rieth L, Williams L, et al. Long-term reliability of Al<sub>2</sub>O<sub>3</sub> and Parylene C bilayer encapsulated Utah electrode array based neural interfaces for chronic implantation. *J Neural Eng*, 2014, 11: 026016
- 106 Fang H, Zhao J N, Yu K J, et al. Ultrathin, transferred layers of thermally grown silicon dioxide as biofluid barriers for biointegrated flexible electronic systems. *Proc Natl Acad Sci USA*, 2016, 113: 11682–11687
- 107 Shen K, Maharbiz M M. Ceramic packages for acoustically coupled neural implants. In: *Proceedings of the 9th International IEEE/EMBS Conference on Neural Engineering (NER)*, 2019. 847–850
- 108 Yao J L, Qiang W J, Wei H, et al. Ultrathin and robust micro-nano composite coating for implantable pressure sensor encapsulation. *ACS Omega*, 2020, 5: 23129–23139
- 109 Bettinger C J, Ecker M, Kozai T D Y, et al. Recent advances in neural interfaces-materials chemistry to clinical translation. *MRS Bull.* 2020, 45: 655–668
- 110 Sharma A, Rieth L, Tathireddy P, et al. Evaluation of the packaging and encapsulation reliability in fully integrated, fully wireless 100 channel Utah Slant electrode array (USEA): implications for long term functionality. *Sens Actuat A-Phys*, 2012, 188: 167–172
- 111 Hwang G T, Im D, Lee S E, et al. In vivo silicon-based flexible radio frequency integrated circuits monolithically encapsulated with biocompatible liquid crystal polymers. *ACS Nano*, 2013, 7: 4545–4553
- 112 Kiourti A, Lee C W L, Chae J, et al. A wireless fully passive neural recording device for unobtrusive neuropotential monitoring. *IEEE Trans Biomed Eng*, 2016, 63: 131–137
- 113 Neely R M, Piech D K, Santacruz S R, et al. Recent advances in neural dust: towards a neural interface platform. *Curr Opin NeuroBiol*, 2018, 50: 64–71
- 114 Luan H W, Zhang Y H. Programmable stimulation and actuation in flexible and stretchable electronics. *Adv Intell Syst*, 2021, 3: 2000228